Systematic investigation of the influencing parameters of an external cavity laser with a quantum dot gain chip

Ehlert, Jannik, Mugnier, Alain, He, Gang, Grillot, Frédéric

Jannik F. Ehlert, Alain Mugnier, Gang He, Frédéric Grillot, "Systematic investigation of the influencing parameters of an external cavity laser with a quantum dot gain chip," Proc. SPIE 11356, Semiconductor Lasers and Laser Dynamics IX, 1135609 (1 April 2020); doi: 10.1117/12.2554553

SPIE.

Event: SPIE Photonics Europe, 2020, Online Only, France

Systematic investigation of the influencing parameters of an external cavity laser with a quantum dot gain chip

Jannik F. Ehlert[a,b], Alain Mugnier[a], Gang He[c], and Frédéric Grillot[b,d]

[a]EXFO Optics, 4 rue Louis de Broglie, 22300 Lannion, France
[b]LTCI, Télécom ParisTech, Institut Polytechnique de Paris, 91120 Palaiseau, France
[c]EXFO Inc., 400 avenue Godin, Québec (Québec), G1M 2K2, Canada
[d]Center for High Technology Materials, University of New-Mexico, Albuquerque, USA

ABSTRACT

External cavity lasers show a variety of uses, for which quantum well semiconductor lasers are already commercially used. Due to the atom-like discrete energy levels, quantum dots exhibit various properties resulting from the three-dimensional confinement of carriers, like high stability against temperature variation, large gain bandwidth, and low-threshold lasing operation. Quantum dots seem to be ideal to address the challenges in the further development of various semiconductor applications, such as high-resolution spectroscopy or broadband optical communication networks, for which a range of spectral and temporal characteristics is required, for instance a narrow spectral linewidth, low intensity noise or wide wavelength tunability. In this view, external cavity quantum dot gain chips can be envisoned to replace the current quantum well technology. Using a semi-analytical rate equation model, we successfully analyze both dynamical and noise properties of an external cavity laser made with quantum dot gain medium, operating under strong optical feedback. This paper investigates the turn-on delay, the relative intensity noise, and the frequency noise and compares them to the case without optical feedback. These numerical investigations of an external cavity quantum dot gain chip provide meaningful building blocks for future fabrication research or for developing high performance device such as wavelength-selective components.

Keywords: External cavity, quantum dots, rate equations, feedback, intensity noise, frequency noise.

1. INTRODUCTION

Quantum dots (QD) have shown a number of promising advantages to be used for lasing emission. For QD lasers, these properties include but are not limited to a low threshold current density,[1,2] large gain bandwidth,[3] a high temperature stability,[4] and a reduced phase noise[5] transforming into a natural spectral linewidth as low as 110 kHz.[6] The latter can even be much further reduced by using a proper external cavity (EC).[7] It has been also widely shown that QD lasers do also have a great potential towards large-scale and low-cost photonic integration by overcoming inherent problems related to standard diode lasers integrated on silicon.[8,9] All these aforementioned properties suggest that a similarly improved performance can be expected with EC QD lasers in terms of operation temperature, output power, noise properties, and tunability.[10,11]

In the context of EC, many types of configurations have been proposed. First, probably the simplest one, consists of an EC semiconductor laser diode with a feedback strength of up to 1%. For any light manipulation, e.g. wavelength selection within the EC, this unintentional feedback is too low to be useful for our case. Additionally, the linewidth is dependent on the feedback phase.[12] Second, an EC semiconductor diode operating with strong feedback of several percents. According to the feedback classification by Tkach et Chraplyvy,[13] the laser operates within regime five when strong optical feedback is considered, meaning that this configuration requires to take into account several round-trips of traveling light inside the EC. The out-coupling facet of the second mirror is a cleaved surface, which is a big disadvantage concerning an instability in laser operation, if not great care is taken on the laser design: Unintentional feedback still needs to be avoided, which would trigger a coherence collapse.[12]

Further author information: (Send correspondence to J.E.)
E-mail: jannik.ehlert@telecom-paristech.fr

Semiconductor Lasers and Laser Dynamics IX, edited by Marc Sciamanna, Rainer Michalzik, Krassimir Panajotov, Sven Höfling, Proceedings of SPIE Vol. 11356, 1135609
 · doi: 10.1117/12.2554553

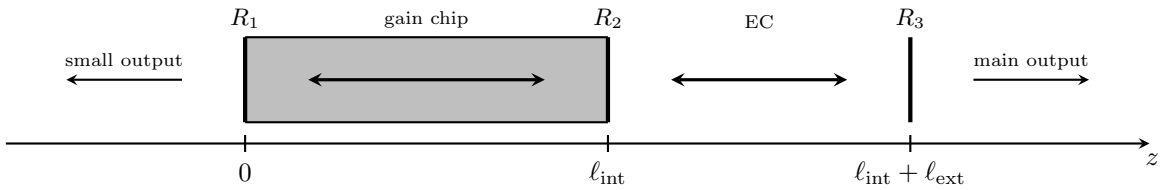

Figure 1. The external cavity (EC) laser has an EC length of ℓ_{ext} and a round trip time of τ_{ext} within mirror reflectivities R. The light output of the gain chip at the rear facet (reflectivity R_1 at $z = 0$) is much smaller than the main output at $z = \ell_{\text{int}} + \ell_{\text{ext}}$. In this work, mirror 2 with reflectivity R_2 is simulated with an anti-reflection coating in EC operation.

Third, a gain chip, i.e., a semiconductor optical amplifier (SOA), can be used as an active medium of a compound cavity. It is this third type with a gain chip that we focus on in this work. Mode solutions are predicted to be stable with narrow linewidths, independent of the feedback phase and additional perturbations.[12,13] For these light sources within compound cavities, several parameters can be investigated such as the influences of bias current, the cavity length, and the power reflectivity of the out-coupling mirror R_2.

This work aims at identifying the influencing parameters driving the properties of an EC QD gain chip. Our simulations are conducted using a semi-analytical approach of the coupled rate equations including both lasing and non-lasing states of the QDs, the Langevin noise sources,[5] as well as the coupling towards the free-space EC with strong optical feedback. We introduce for the first time this model to EC QD lasers by investigating the fundamental properties such as the turn-on delay, the relative intensity noise, and the frequency noise. We also compare the simulation results to the case without optical feedback and shed the light on the importance of the EC length as well as the power reflectivity of the out-coupling mirror R_2. These numerical investigations of an EC QD gain chip provide initial building blocks for future fabrication research or for developing high performance devices with wavelength-selective components.

2. SEMI-ANALYTICAL MODEL

The laser under study is represented in Figure 1. It consists of a QD gain chip operating in free-space. The light in the EC of length ℓ_{ext} shows a round trip time of τ_{ext}, reflected by the external mirror (power reflectivity $R_3 = 0.32$). The light output of the gain chip at the rear facet (reflectivity $R_1 = 0.95$ at $z = 0$) is much smaller than the main output at $z = \ell_{\text{int}} + \ell_{\text{ext}}$. In this work, mirror 2 with a power reflectivity R_2 has a antireflection (AR) coating in the EC operation. In practice, we assume that the effective reflectivity of the front facet can possibly be enhanced by the angled waveguide design which is used for making the SOA gain chip. The numerical model holds under the assumption that the active region consists of only one QD ensemble, where QDs are interconnected by a wetting layer (reservoir RS). The QD ensemble includes two energy levels: a two-fold degenerate ground state (GS) and a four-fold degenerate excited state (ES). The QDs are assumed to be always neutral, electrons and holes are treated as electron-hole pairs, which means that the system is in excitonic energy state. Carriers are supposed to be injected directly from the contacts into the RS level, so the carrier dynamics in the barrier is not taken into account in the model.

Following the sketch of Figure 2 and the notation of Wang et al.,[5] $\tau_{\text{ES}}^{\text{RS}}$ and $\tau_{\text{RS}}^{\text{ES}}$ represent the capture time from RS to ES and the relaxation time in opposite direction from ES to RS, respectively. $\tau_{\text{GS}}^{\text{ES}}$ and $\tau_{\text{ES}}^{\text{GS}}$ are the escape times from ES to GS and vice versa, respectively. Spontaneous emission is represented for each level by $\tau_{\text{RS,ES,GS}}^{\text{spon}}$. The carrier escape from GS to RS has been neglected.[14] The three number rate equations on carriers are as follows.

$$\frac{\mathrm{d}N_{\text{RS}}}{\mathrm{d}t} = \frac{I}{q} + \frac{N_{\text{ES}}}{\tau_{\text{RS}}^{\text{ES}}} - \frac{N_{\text{RS}}}{\tau_{\text{ES}}^{\text{RS}}} f_{\text{ES}} - \frac{N_{\text{RS}}}{\tau_{\text{RS}}^{\text{spon}}} + F_{\text{RS}} \tag{1}$$

$$\frac{\mathrm{d}N_{\text{ES}}}{\mathrm{d}t} = \frac{N_{\text{RS}}}{\tau_{\text{ES}}^{\text{RS}}} f_{\text{ES}} + \frac{N_{\text{GS}}}{\tau_{\text{ES}}^{\text{GS}}} f_{\text{ES}} - \frac{N_{\text{ES}}}{\tau_{\text{RS}}^{\text{ES}}} - \frac{N_{\text{ES}}}{\tau_{\text{GS}}^{\text{ES}}} f_{\text{GS}} - \frac{N_{\text{ES}}}{\tau_{\text{ES}}^{\text{spon}}} + F_{\text{ES}} \tag{2}$$

$$\frac{\mathrm{d}N_{\text{GS}}}{\mathrm{d}t} = \frac{N_{\text{ES}}}{\tau_{\text{GS}}^{\text{ES}}} f_{\text{GS}} - \frac{N_{\text{GS}}}{\tau_{\text{ES}}^{\text{GS}}} f_{\text{ES}} - \frac{N_{\text{GS}}}{\tau_{\text{GS}}^{\text{spon}}} - \Gamma_p g v_g N_p + F_{\text{GS}} \tag{3}$$

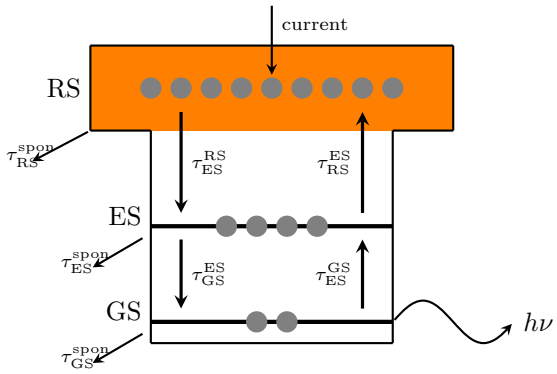

Figure 2. The electronic structure indicates the carrier dynamics including a reservoir state (RS), an excited state (ES), and a ground state (GS), transition times between levels, and spontaneous emission times.[18]

where $N_{\mathrm{RS}}, N_{\mathrm{ES}}$, and N_{GS} are the carrier numbers in RS, ES, and GS, respectively; I the bias current; $F_{\mathrm{RS,ES,GS}}$ are the Langevin noise sources for the carriers in RS, ES, and GS, respectively; β_{SP} the spontaneous emission factor; v_g the group velocity; f_{ES} and f_{GS} the Pauli blocking factors; and q the elementary charge of carriers. All symbols can be found in Table 1. The photon number and the phase equations incorporating the feedback terms read as follows:[15,16]

$$\frac{\mathrm{d}N_p}{\mathrm{d}t} = \left(\Gamma_p g v_g - \frac{1}{\tau_p}\right) N_p + \beta_{SP}\frac{N_{\mathrm{GS}}}{\tau_{\mathrm{GS}}^{\mathrm{spon}}} + 2\kappa\sqrt{N_p(t)\,N_p(t-\tau_{\mathrm{ext}})}\cos\left(\omega_0\tau_{\mathrm{ext}} + \phi(t) - \phi(t-\tau_{\mathrm{ext}})\right) + F_{N_p} \tag{4}$$

$$\frac{\mathrm{d}\phi}{\mathrm{d}t} = \frac{\alpha_H}{2}\left(\Gamma_p g v_g - \frac{1}{\tau_p}\right) - \kappa\sqrt{\frac{N_p(t-\tau_{\mathrm{ext}})}{N_p(t)}}\sin\left(\omega_0\tau_{\mathrm{ext}} + \phi(t) - \phi(t-\tau_{\mathrm{ext}})\right) + F_\phi \tag{5}$$

where τ_{ext} is the round-trip time in the free space EC of length ℓ_{ext}, κ the feedback term, α_H the linewidth enhancement factor, F_{N_p} and F_ϕ the Langevin noise sources for photon numbers N_p and the phase ϕ respectively, and ω_0 the single mode angular lasing frequency. The GS gain,[16] the feedback strength,[17] and the photon lifetime are expressed respectively as

$$g = \frac{a_{\mathrm{GS}}\left(N_{\mathrm{GS}} - N_B\right)}{V_{QD}(1 + \varepsilon N_p/V_p)} \tag{6}$$

$$\kappa = \sqrt{\frac{R_2}{R_3}}\cdot\frac{1}{\tau_{\mathrm{ext}}} \tag{7}$$

$$\tau_p = \left(c\alpha_{in} - \frac{c\cdot\ln(R_1R_3)}{2(n_g\ell_{\mathrm{int}} + \ell_{\mathrm{ext}})}\right)^{-1} \tag{8}$$

where a_{GS} is the differential gain associated to the GS transition, ε the gain compression factor, V_p the confinement volume, N_B the total dot number, n_g the refractive index in the active region, α_{in} the internal losses, c the speed of light in vacuum, and ℓ_{int} the cavity length of the gain chip.

After linearizing the above rate equations through a small signal analysis and using Taylor polynomial approximations, neglecting higher order terms gives the following matrix:[16,19]

$$\begin{bmatrix} \gamma_{11}+j\omega & -\gamma_{12} & 0 & 0 & 0 \\ -\gamma_{21} & \gamma_{22}+j\omega & -\gamma_{23} & 0 & 0 \\ 0 & -\gamma_{32} & \gamma_{33}+j\omega & -\gamma_{34} & 0 \\ 0 & 0 & -\gamma_{43} & \gamma_{44}+j\omega & -\gamma_{45} \\ 0 & 0 & -\gamma_{53} & -\gamma_{54} & \gamma_{55}+j\omega \end{bmatrix} \cdot \begin{bmatrix} \mathrm{d}N_{\mathrm{RS}} \\ \mathrm{d}N_{\mathrm{ES}} \\ \mathrm{d}N_{\mathrm{GS}} \\ \mathrm{d}N_p \\ \mathrm{d}\phi \end{bmatrix} = \frac{\mathrm{d}I}{q}\begin{bmatrix} 1 \\ 0 \\ 0 \\ 0 \\ 0 \end{bmatrix} \tag{9}$$

with γ_{ij} the matrix elements,[16] and ω the modulation angular frequency. The relaxation oscillation frequency f_{R} and the damping factor γ can be obtained either from the RIN spectrum or from the calculation based on the above matrix elements.[18]

Table 1. Material and laser parameters[4,16,18]

symbol	definition	value	symbol	definition
a_{GS}	GS differential gain	$5 \cdot 10^{-15}\,\mathrm{cm}^2$	f_{ES}	ES occupation probability
α_H	linewidth enhancement factor	1	f_{GS}	GS occupation probability
α_{in}	loss of internal cavity	$5\,\mathrm{cm}^{-1}$	g	gain
β_{SP}	spontaneous emission factor	10^{-4}	I	bias current
Γ_p	optical confinement factor	0.06	ℓ_{ext}	external cavity length
E_{RS}	RS energy	0.97 eV	N_B	total dot number
E_{ES}	ES energy	0.87 eV	N_{ES}	number of ES charge carriers
E_{GS}	GS energy	0.82 eV	N_{GS}	number of GS charge carriers
ε	gain compression	$0\,\mathrm{cm}^3$	N_{RS}	number of RS charge carriers
h_{QD}	QD thickness/layer height	5 nm	N_p	number of photons
$\ell_{\mathrm{int}} \times W$	active medium length × width	1.1 mm × 3 μm	$\Delta\nu$	optical linewidth[22]
N	number of QD layers	5	ϕ	phase
n_g	refractive index (internal cavity)	3.27	$R_{1,2,3}$	power reflectivity of mirrors
T	temperature	290 K	τ_{ext}	external cavity round-trip time
$\tau_{\mathrm{ES}}^{\mathrm{RS}}$	RS to ES capture time	25.1 ps	τ_p	photon lifetime
$\tau_{\mathrm{GS}}^{\mathrm{ES}}$	ES to GS relaxation time	11.6 ps	v_g	group velocity
$\tau_{\mathrm{RS}}^{\mathrm{ES}}$	ES to RS escape time	5.8 ns	V_p	confinement volume (V_{QD}/Γ_p)
$\tau_{\mathrm{ES}}^{\mathrm{GS}}$	GS to ES escape time	42.9 ps	V_{QD}	active region volume
$\tau_{\mathrm{RS,ES}}^{\mathrm{spon}}$	RS/ES spontaneous emission time	0.5 ns	ω	current modulation angular frequency
$\tau_{\mathrm{GS}}^{\mathrm{spon}}$	GS spontaneous emission time	1.2 ns		

In the following, we analyze the properties of the EC QD laser operating under strong optical feedback. In other words, although the feedback strength is much higher than 1% of the emitted light, only one round-trip is assumed since the compound cavity is made with an AR coated front facet (mirror 2), which reflects almost nothing back into the internal cavity. This last effect is also strengthened by the tilted face of the SOA gain chip. In addition to that, it was shown that when the product of the feedback strength κ and the EC round-trip time τ_{ext} is small enough, a single round-trip can be considered, which is exactly what happens in the case under study.[20]

The noise analysis is based on the modulation frequency-dependent relative intensity noise

$$\mathrm{RIN}(\omega) = \frac{|\delta N_p(\omega)|^2}{N_p^2} \tag{10}$$

and the frequency noise (FN).[4] Simulations include the Langevin noise sources for the carriers $F_{\mathrm{RS,ES,GS}}$, as well as for photons F_{N_p} and for the phase F_ϕ.[4,16] Simulations are conducted with MATLAB© for which the used function for solving the differential partial equations with delayed feedback τ_{ext} is `dde23`.[21]

3. RESULTS AND DISCUSSION

In this section, the model is applied to the EC QD gain chip with a power reflectivity of the out-coupling mirror $R_2 = 10^{-4}$. Simulation focuses on the dynamic and noise properties assuming different values of the EC length. All performances are compared to a free running case, i.e., without optical feedback ($R_3 = 0$). In such a case, the free-running laser keeps a high-reflective coating on the rear facet ($R_1 = 0.95$) whereas the front one remains as-cleaved ($R_2 = 0.32$). Other parameters used in the simulations are displayed in Table 1.

At first, the carrier number in the GS level is calculated (Figure 3a) with respect to the injected current and for different values of ℓ_{ext}, i.e., 6 mm (red), 1.5 cm (yellow), 3 cm (violet), 6 cm (green), and 9 cm (light blue). Simulations show that the GS population is clamped for a certain injected current, which leads to the occurrence of the GS lasing emission. Compared to the free-running case, the EC QD laser exhibits a reduced carrier number at threshold, which means that the threshold current is also slightly decreased. This decrease is confirmed by the simulated light-current characteristics (Figure 3b). Let us stress that in addition to that, an EC

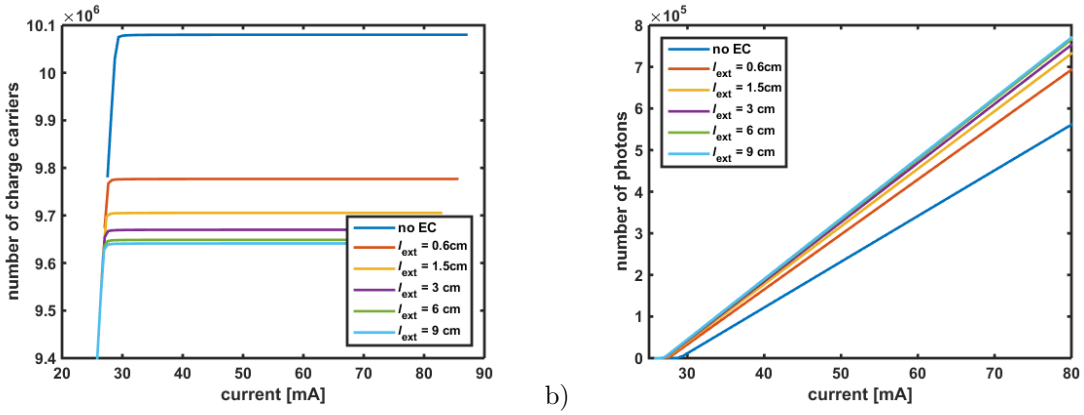

a) b)

Figure 3. a) GS carrier number and b) Photon number for no EC (dark blue), and different EC lengths: 6 mm (red), 1.5 cm (yellow), 3 cm (violet), 6 cm (green), and 9 cm (light blue).

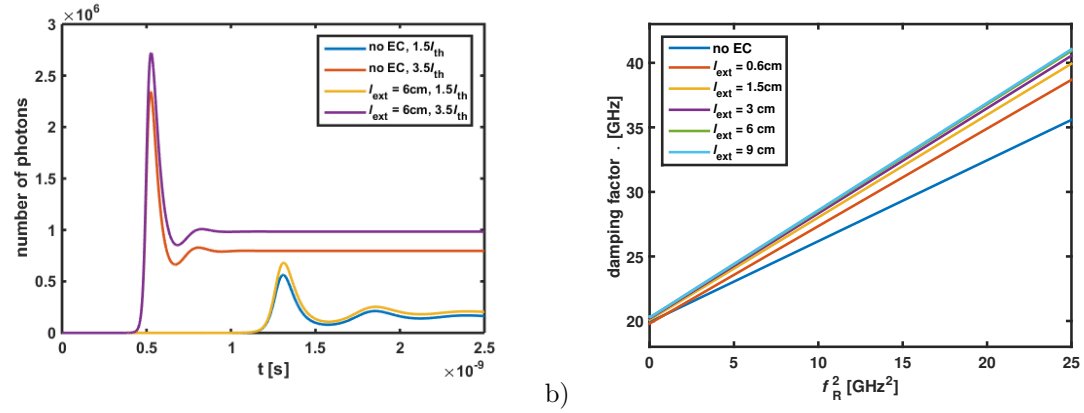

a) b)

Figure 4. a) Turn-on delay b) Damping factor γ as a function of the squared relaxation oscillation frequency f_R^2 for no EC (dark blue), and different EC lengths: 6 mm (red), 1.5 cm (yellow), 3 cm (violet), 6 cm (green), and 9 cm (light blue).

laser provides a higher photon number, meaning a larger output power, which is important for high performance wavelength-selective components. For instance, with $\ell_{\text{ext}} = 3$ cm, the threshold current decreases from 29 mA to 27 mA, whereas the maximum photon number at 80 mA is found to be enhanced from about 5.6×10^5 (without EC) to more than 7.7×10^5 (for $\ell_{\text{ext}} = 9$ cm).

Then, the evolution of the turn-on delay properties illustrates two main observations at 1.5 and 3.5 times the threshold current I_{th} (Figure 4a). With the increase of the injected current, the delay time becomes shorter which means that the carrier lifetime is decreased. Both the relaxation oscillation frequency and the damping factor increase with the current which is in line with prior studies.[18] The oscillation frequencies at 1.5 and $3.5 \times I_{\text{th}}$ are 2.7 GHz and 6.2 GHz, respectively. Second, with an EC, the number of photons is increased beyond the free-running value which is in agreement with the aforementioned simulations.

Then, the damping factor is displayed as a function of the squared relaxation oscillation frequency f_R (Figure 4b). First, it is found to scale up with the relaxation frequency through the injected current and exhibits higher values than those observed in quantum well lasers[18] hence ranging from 20 GHz to more that 30 GHz depending on the bias conditions. Second, it also strongly depends on the EC length hence being enhanced by several GHz at larger values of ℓ_{ext}, whereas f_R is reduced. This effect results from the compound cavity made with a front-facet AR coating on the gain chip, which means that the photon lifetime increases with the total cavity length, so does the damping.

Simulations of the RIN and FN characteristics are now depicted in Figure 5 for three different normalized bias currents: $1.5 \times I_{\text{th}}$ (upper blue curves), $2.5 \times I_{\text{th}}$ (center red curves), and $3.5 \times I_{\text{th}}$ (lower yellow curves) and at a fixed EC length of $\ell_{\text{ext}} = 6$ cm. At low frequencies below the relaxation peak, a constant RIN value is expected,[4]

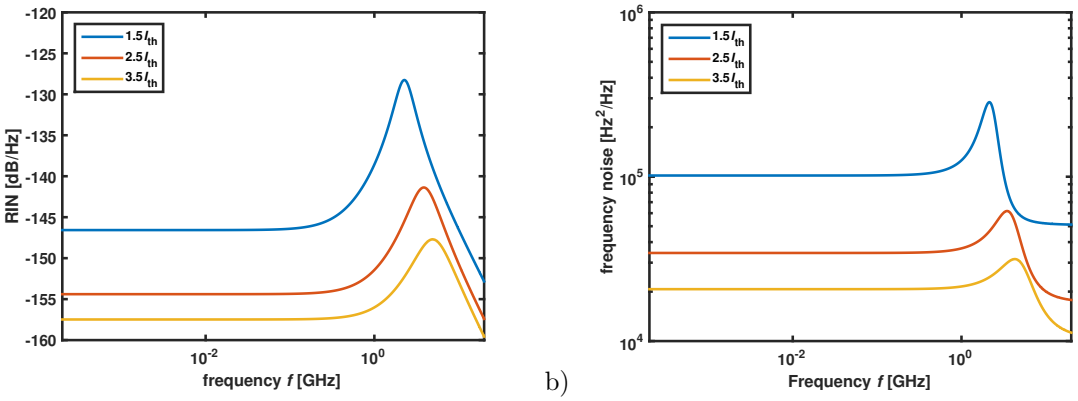

a) b)

Figure 5. a) RIN and b) FN spectra calculated for three different normalized bias currents $1.5 \times I_{\mathrm{th}}$ (upper blue curves), $2.5 \times I_{\mathrm{th}}$ (center red curves), and $3.5 \times I_{\mathrm{th}}$ (lower yellow curves). The length of the EC is fixed to $\ell_{\mathrm{ext}} = 6\,\mathrm{cm}$.

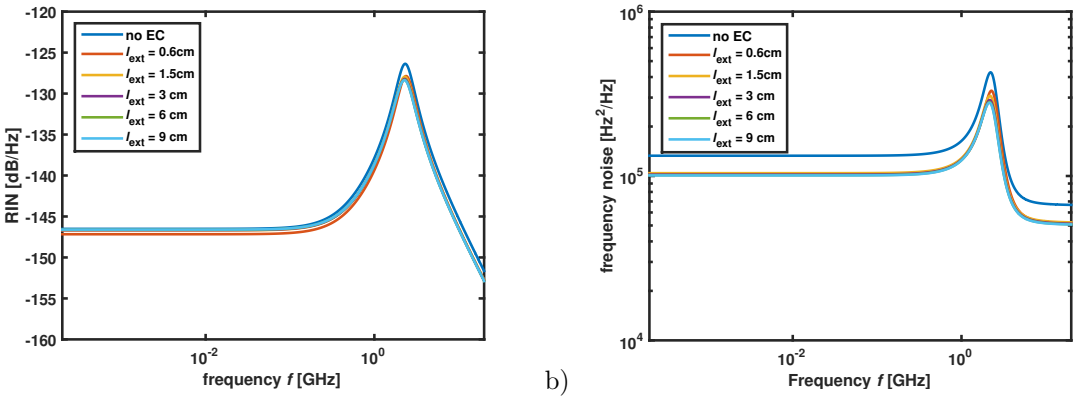

a) b)

Figure 6. Simulations at $1.5 \times I_{\mathrm{th}}$ of a) the RIN and b) the FN with respect to the EC length.

which is confirmed here. Besides, the RIN at 1 MHz drops from –146.5 dB/Hz at $1.5 \times I_{\mathrm{th}}$ down to –157.5 dB/Hz at $3.5 \times I_{\mathrm{th}}$. Yet at higher frequencies than the relaxation peak, the RIN decreases strongly and reaches its smallest value. For instance, at 20 GHz, it drops down to –152.8 dB/Hz at $1.5 \times I_{\mathrm{th}}$ and to –159.6 dB/Hz at $3.5 \times I_{\mathrm{th}}$. On top of that, our simulations also show that the RIN spectrum is hardly influenced by a modification of the EC length. Contrary to the work performed by Hisham et al.,[23] no significant change is observed in Figure 6a. Such a difference can be attributed to the photon lifetime τ_p which is calculated in our case by considering the photon traveling in the complete cavity. In other words, the reflectivity of the second mirror R_2 can be regarded as a perturbation with respect to the total cavity $\ell_{\mathrm{int}} + \ell_{\mathrm{ext}}$. Therefore, any change in ℓ_{ext} is found to have a much lower influence on the RIN. As expected from the RIN spectrum, the relaxation oscillation frequency, which roughly correspond to the relaxation peak, is almost not affected either.

Finally, the optical linewidth is also evaluated from the FN[5,22] given by $\Delta\nu = 2\pi \mathrm{FN}|_{f \ll f_R}$. In Figure 5b, the FN decreases with the bias current due to the coherent photon population building inside the cavity. Assuming an EC of $\ell_{\mathrm{ext}} = 6\,\mathrm{cm}$, the FN is about 10^5 Hz^2/Hz at $1.5 \times I_{\mathrm{th}}$ hence resulting in a spectral linewidth of about 640 kHz, which is further decreased down to about 130 kHz when the bias current is at $3.5 \times I_{\mathrm{th}}$.

Simulations unveil the impact of an EC (Figure 6): It leads to a FN reduction, but surprisingly, the RIN is found not to be affected which needs further analysis at this stage. At the same current of $1.5 \times I_{\mathrm{th}}$ the free-running configuration leads to a FN of 1.33×10^5 Hz^2/Hz hence resulting in a broader spectral linewidth of about 840 kHz, which is further decreased down to about 170 kHz at $3.5 \times I_{\mathrm{th}}$. As for the impact of the AR coating, simulations show that no major change is unveiled on the RIN spectrum and on the damping factor (Figure 7), which proves that the EC QD gain chip exhibits a very good tolerance against any AR coating impairment.

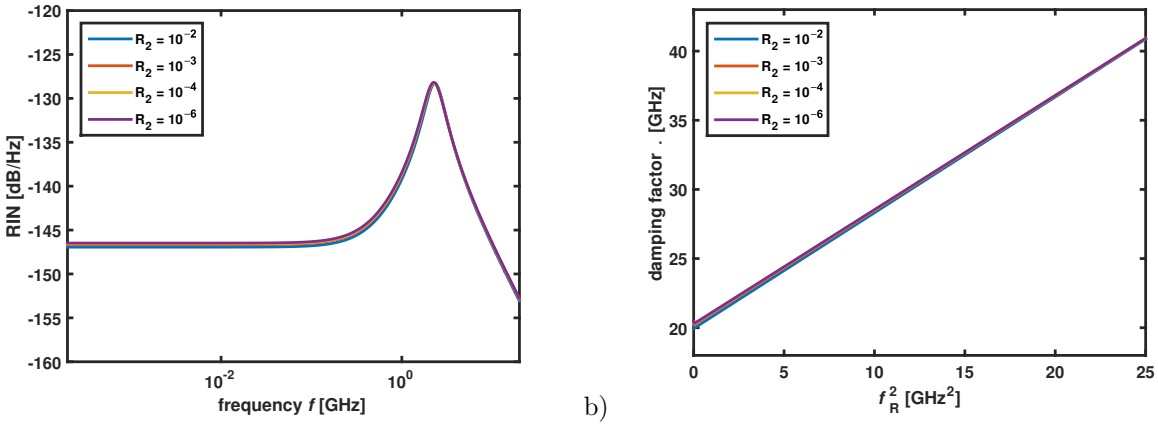

a) b)

Figure 7. Impact of the AR coating impairment on the a) RIN and b) damping factor assuming a power reflectivity R_2 ranging from 10^{-2}, 10^{-3}, 10^{-4}, to 10^{-6}. The length of the EC is fixed to $\ell_{\text{ext}} = 6\,\text{cm}$.

4. CONCLUSIONS

To summarize, a rate equation model is successfully applied to an QD gain chip-based EC laser. It is based on a semi-analytical approach using a small signal analysis and numerical evaluation. The simulation unveil the importance of the design of the EC on the dynamic and noise characteristics. Several possible conclusions can be drawn from the low influence on the AR coated mirror towards the EC. First, given that a power reflectivity of 10^{-4} is already attainable, there is no need to go to lower values. Second, variations in the AR can be allowed without altering the device performance in terms of photon number, thus output power. Another key parameter shows that the EC length and thus the photon lifetime is barely influenced by a variation in length of around 6 cm. Therefore, all of these initial investigations give initial design guidelines for the realization of future QD gain chip-based EC lasers.

5. ACKNOWLEDGMENTS

The authors are grateful for R. Lebref and F. Couny for helpful comments and encouragement. This work was funded by EXFO Optics and ANRT under the CIFRE program 2018/0793.

REFERENCES

[1] Deppe, D. G., Shavritranuruk, K., Ozgur, G., Chen, H., and Freisem, S., "Quantum dot laser diode with low threshold and low internal loss," *Electronics Letters* **45**(1), 54–56 (2009).

[2] Liu, G. T., Stintz, A., Li, H., Malloy, K. J., and Lester, L. F., "Extremely low room-temperature threshold current density diode lasers using InAs dots in $In_{0.15}Ga_{0.85}As$ quantum well," *Electronics Letters* **35**(14), 1163–1165 (1999).

[3] Varangis, P. M., Li, H., Liu, G. T., Newell, T. C., Stintz, A., Fuchs, B., Malloy, K. J., and Lester, L. F., "Low-threshold quantum dot lasers with 201 nm tuning range," *Electronics Letters* **36**(18), 1544–1545 (2000).

[4] Duan, J., Wang, X., Zhou, Y., Wanga, C., and Grillot, F., "Carrier-Noise Enhanced Relative Intensity Noise of Quantum Dot Lasers," *IEEE Journal of Quantum Electronics* **54**(6), 1–7 (2018).

[5] Wang, C., Zhuang, J.-P., Grillot, F., and Chan, S.-C., "Contribution of off-resonant states to the phase noise of quantum dot lasers," *Optics Express* **24**, 29872–29881 (2016).

[6] Becker, A., Sichkovskyi, V., Bjelica, M., Eyal, O., Baum, P., Rippien, A., Schnabel, F., Witzigmann, B., Eisenstein, G., and Reithmaier, J. P., "Narrow-linewidth 1.5-μm quantum dot distributed feedback lasers," *Proceedings SPIE* **9767**(Novel In-Plane Semiconductor Lasers XV), 97670Q (2016).

[7] Kita, T., Tang, R., and Yamada, H., "Narrow spectral linewidth silicon photonic wavelength tunable laser diode for digital coherent communication system," *IEEE Journal of Selected Topics in Quantum Electronics* **22**(6), 23–34 (2016).

[8] Arakawa, Y., "Quantum dot lasers for silicon photonics," in [*2016 21st OptoElectronics and Communications Conference (OECC) Held Jointly with 2016 International Conference on Photonics in Switching (PS)*], 1–2 (2016).

[9] Chen, S., Li, W., Wu, J., Jiang, Q., Tang, M., Shutts, S., Elliott, S. N., Sobiesierski, A., Seeds, A. J., Ross, I., Smowton, P. M., and Liu, H., "Electrically pumped continuous-wave III–V quantum dot lasers on silicon," *Nature Photonics* **10**(5), 307–311 (2016).

[10] Li, S. G., Gong, Q., Cao, C. F., Wang, X. Z., Yan, J. Y., Wang, Y., and Wang, H. L., "A review of external cavity-coupled quantum dot lasers," *Optical and Quantum Electronics* **46**(5), 623–640 (2014).

[11] Nevsky, A. Y., Bressel, U., Ernsting, I., Eisele, C., Okhapkin, M., Schiller, S., Gubenko, A., Livshits, D., Mikhrin, S., Krestnikov, I., and Kovsh, A., "A narrow-line-width external cavity quantum dot laser for high-resolution spectroscopy in the near-infrared and yellow spectral ranges," *Applied Physics B* **92**(4), 501–507 (2008).

[12] Coldren, L. A., Corzine, S. W., and Mašanović, M. L., "Dynamic Effects," in [*Diode Lasers and Photonic Integrated Circuits*], 247–333, Wiley-Blackwell, 2 ed. (2012).

[13] Tkach, R. and Chraplyvy, A., "Regimes of feedback effects in 1.5μm distributed feedback lasers," *Journal of Lightwave Technology* **4**(11), 1655–1661 (1986).

[14] Veselinov, K., Grillot, F., Cornet, C., Even, J., Bekiarski, A., Gioannini, M., and Loualiche, S., "Analysis of the double laser emission occurring in 1.55-μm InAs-InP (113)B quantum-dot lasers," *IEEE Journal of Quantum Electronics* **43**(9), 810–816 (2007).

[15] Lang, R. and Kobayashi, K., "External optical feedback effects on semiconductor injection laser properties," *IEEE Journal of Quantum Electronics* **16**(3), 347–355 (1980).

[16] Grillot, F., Wang, C., Naderi, N. A., and Even, J., "Modulation Properties of Self-Injected Quantum-Dot Semiconductor Diode Lasers," *IEEE Journal of Selected Topics in Quantum Electronics* **19**(4), 1900812–1900812 (2013).

[17] Columbo, L., Bovington, J., Romero-Garcia, S., Siriani, D. F., and Gioannini, M., "Efficient and Optical Feedback Tolerant Hybrid Laser Design for Silicon Photonics Applications," *IEEE Journal of Selected Topics in Quantum Electronics* **26**(2), 1–10 (2020).

[18] Wang, C., Grillot, F., and Even, J., "Impacts of Wetting Layer and Excited State on the Modulation Response of Quantum-Dot Lasers," *IEEE Journal of Quantum Electronics* **48**(9), 1144–1150 (2012).

[19] Helms, J. and Petermann, K., "Microwave modulation of laser diodes with optical feedback," *Journal of Lightwave Technology* **9**(4), 468–476 (1991).

[20] Ye, C., [*Tunable External Cavity Diode Lasers*], World Scientific (2004).

[21] MATLAB, [*8.4.0.150421 (R2014b)*], The MathWorks Inc., Natick, Massachusetts (2014).

[22] Ohtsubo, J., [*Semiconductor Lasers*], Springer (2012).

[23] Hisham, H. K., Abas, A. F., Mahdiraji, G. A., Mahdi, M. A., and Noor, A. S. M., "Relative Intensity Noise Reduction by Optimizing Fiber Grating Fabry–Perot Laser Parameters," *IEEE Journal of Quantum Electronics* **48**(3), 375–383 (2012).